Journal of Colloid and Interface Science 327 (2008) 169–179

Contents lists available at ScienceDirect

Journal of Colloid and Interface Science

www.elsevier.com/locate/jcis

Method for analysis of the composition of acid soaps by electrolytic conductivity measurements

Peter A. Kralchevsky [a,*], Mariana P. Boneva [a], Krassimir D. Danov [a], Kavssery P. Ananthapadmanabhan [b], Alex Lips [b]

[a] Laboratory of Chemical Physics and Engineering, Faculty of Chemistry, Sofia University, 1164 Sofia, Bulgaria
[b] Unilever Research and Development, Trumbull, CT 06611, USA

ARTICLE INFO

Article history:
Received 17 May 2008
Accepted 1 August 2008
Available online 7 August 2008

Keywords:
Carboxylate soap solutions
Acid-soap crystallites, stoichiometry
Potassium myristate
Electrolytic conductivity
Molar ionic conductances

ABSTRACT

Here, we propose a method for determining the stoichiometry of acid-soap crystallites. The method is based on dissolving the crystallites in water at an appropriate working temperature, followed by measurement of the electrolytic conductivity of the obtained solutions. The working temperature is chosen in such a way that the only precipitate in the solutions is that of carboxylic acid, whereas the carboxylate salt is dissociated, and its content in the dissolved crystals determines the solution's conductivity. In the theoretical model for data interpretation, we took into account the dependence of the molar conductance on the ionic strength. The method was applied for determining the stoichiometry of acid-soap crystals collected from solutions of potassium myristate (tetradecanoate) at 25 °C. The crystals were dissolved in water at working temperature of 40 °C, at which the conductivity was measured. The stoichiometry of all samples determined in the present study coincides with that independently obtained by another method that is based on *in situ* pH measurements.

1. Introduction

The sodium and potassium carboxylates (dodecanoates, tetradecanoates, hexadecanoates, and octadecanoates, which are popular, respectively, as laurates, myristates, palmitates, and stearates) have a broad application in many consumer products like soap bars; cleaning products; cosmetics; facial cleaners; shaving creams, and deodorants [1–3]. The dissolving of carboxylates in water is accompanied by increase of the solution's pH due to the spontaneous hydrolysis (protonation) of the carboxylate anion [4]:

$$Z^- + H_2O \leftrightarrow HZ + OH^-.$$

Here we use the notations in Ref. [4], viz. Z^- is carboxylate anion, and HZ is non-dissociated carboxylic acid. The non-dissociated HZ with 12 and more carbon atoms is weakly soluble in water and forms crystalline precipitates at relatively low carboxylate concentrations ($\leqslant 10^{-5}$ M). Moreover, the hydrogen-bonding interaction between the carboxylic-acid molecules and carboxylate anions leads to the formation of *j*:*n* acid-soap complexes that also form crystalline precipitates [5–9]:

$$jHZ + nZ^- + nM^+ \leftrightarrow (HZ)_j(MZ)_n.$$

Here, M^+ is a metal cation (usually Na^+ or K^+), and $(HZ)_j(MZ)_n$ is the acid soap. The acid soaps were investigated by Ekwall et al. [5–7,10–12], McBain et al. [8,9], and in subsequent studies [3,4,13–21]. Soaps of different stoichiometry, $j{:}n = 1{:}1, 1{:}2, 2{:}1, 3{:}2, 4{:}1$, etc., have been experimentally detected [3,12–14,19–21]. In fact, the turbidity of the soap solutions is due to the formation of fine (micrometer and submicrometer) *j*:*n* acid-soap crystallites.

As mentioned above, the solution's pH increases with the rise of the total input concentration of carboxylate, c_t. For the acid-soap precipitates, the ratio n/j increases with the rise of c_t; its value can be determined from the slope of the experimental pH-vs-c_t dependence, or from plots of precipitate characteristic functions [4,21]. Above a certain threshold concentration, separation of MZ from the solution begins in the form of either MZ crystallites [21] or micelles [22]. In the case of two coexisting solids, viz. acid-soap and MZ crystallites, the solution's pH remains constant (independent of c_t) in agreement with the Gibbs phase rule [4,21]. In the case of coexisting *j*:*n* acid soap and micelles, the soap stoichiometry and micelle charge can be determined by analysis of experimental data from parallel *in situ* measurements of pH and conductivity [22].

Sometimes, the results obtained by *in situ* measurements with the carboxylate solutions can be uncertain. For example, the concentration range with a given acid-soap precipitate could be rather narrow, or the value of a given solubility product, which is needed to interpret the data, is unknown. For this reason, it is desirable to determine the acid-soap stoichiometry by using an independent method. We could separate crystallites from a given carboxylate solution and to subject them to chemical analysis. One analyti-

* Corresponding author. Fax: +359 2 962 5643.
E-mail address: pk@lcpe.uni-sofia.bg (P.A. Kralchevsky).

0021-9797/$ – see front matter
doi:10.1016/j.jcis.2008.08.006

cal method, which has been applied to identify acid soaps, is the IR spectroscopy [3,15,23]. One difficulty with this method is the lack of reference spectra for the whole variety of possible j:n acid soaps.

Here, we propose another direct method for analyzing the stoichiometry of $(HZ)_j(MZ)_n$ acid soaps. The principle of this method is the following. Acid-soap crystallites of unknown stoichiometry are collected from a carboxylate solution at a given temperature. Further, these crystallites are dissolved in water at a higher temperature, at which HZ is insoluble, but MZ is dissociated to M^+ and Z^- ions. By measuring the conductivity of the latter solution, we can determine the stoichiometry of the dissolved acid soap.

The paper is organized as follows. In Section 2 we describe the proposed method. In Section 3 we quantify the dependence of the conductivity of MZ-solutions on the MZ concentration, for the case of potassium myristate (KMy) by using an approach based on the studies by Walden et al. [24,25]. Finally, in Section 4 we present experimental data and their interpretation; demonstrate how the proposed method works, and discuss the limits of its applicability.

2. Description of the proposed method

We assume that a sample of solid (crystalline) acid soap is available. This sample could be obtained by taking crystallites out of a carboxylate solution at a given temperature and carboxylate concentration (details in Section 4 below). Our aim is to determine the stoichiometry of the investigated sample of $(HZ)_j(MZ)_n$ acid soap. For this goal, we propose the following working procedure.

First, we dissolve the acid-soap crystallites in water at appropriate working conditions. The latter are chosen in such a way that the only precipitate in the solution is that of HZ, whereas MZ is dissociated to M^+ and Z^- ions.

Second, the electrolytic conductivity, κ, of the solutions is measured. κ will be greater if the content of MZ in the $(HZ)_j(MZ)_n$ acid soap is greater. In this way, by quantitative data analysis, we can determine the stoichiometry, j:n, of the acid soap (see below).

To illustrate the application of this method, in the present study we work with potassium myristate (KMy). To select the working conditions, we measured the dependence of pH of aqueous KMy solutions on the total input concentration of KMy, c_t, at 40 °C; see Fig. 1. The data in Fig. 1 exhibit a break at $c_t \approx 7.5$ mM. For $c_t < 7.5$ mM, the slope of the pH vs $\log(c_t)$ plot is +1 (the straight line in Fig. 1), which indicates precipitation of HZ crystallites [4,21]; see Section 5.1 for details. At $c_t > 7.5$ mM, the solutions contain KMy micelles that coexist with acid-soap crystallites; this has been proven by combined pH, conductivity and oil-solubilization measurements in Ref. [22].

In view of the data in Fig. 1, we choose our working conditions (for KMy) to be $T = 40$ °C and $c_t < 7.5$ mM. Under these conditions, the only precipitate in the solution is that of HMy, whereas KMy is dissociated to K^+ and My^- ions.

By using equilibrium relationships for carboxylate solutions [4,21,22], one can prove that in the concentration zone, where only HZ precipitate is present (no micelles), the concentrations of carboxylate anions and metal cations, c_Z and c_M, are related as follows:

$$c_Z \approx c_M\left(1 - \frac{K_W}{K_{HZ}}\right) \tag{1}$$

(no added acid). K_{HZ} is the solubility product of the carboxylic acid (HZ) and K_W is the dissociation constant of water. For the considered carboxylates we have $K_W/K_{HZ} \ll 1$, which means that $c_Z \approx c_M$. In other words, the amount of the HZ precipitate is much smaller than the amounts of the M^+ and Z^- ions in the solution; the concentrations of the latter two types of ions are approximately equal to each other, and to the ionic strength, I, of the carboxylate solution:

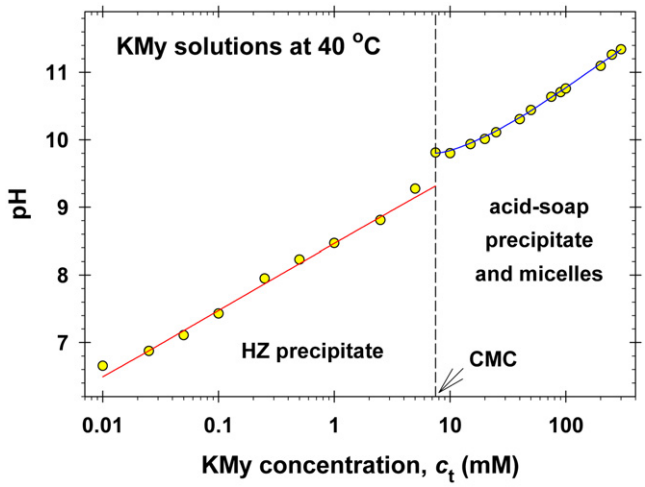

Fig. 1. Plot of experimental data for the pH of potassium myristate (KMy) solutions vs the total input KMy concentration, c_t, at temperature 40 °C. The straight line at $c_t <$ CMC has slope = +1, which indicates the presence of HZ precipitate [4,21]. For $c_t >$ CMC, MZ micelles coexist with $(HZ)_1(MZ)_2$ acid-soap crystallites [22].

$$c_Z \approx c_M = c_t \approx I \quad \left(I \equiv \frac{1}{2}\sum_i z_i^2 c_i\right) \tag{2}$$

(c_i and z_i denote concentrations and valences of the ionic species). Equation (2) is violated at concentrations higher than a given threshold concentration that corresponds to the beginning of separation of neutral soap (MZ) in the form of MZ crystallites as it is for NaMy, see Ref. [21], or in the form of MZ micelles as it is for KMy, see Fig. 1; details can be found in Ref. [22]. As already mentioned, to determine the stoichiometry of the acid-soap samples, we will work at sufficiently low concentrations and at a sufficiently high temperature, so that the carboxylate solutions contain only HZ precipitate, and Eq. (2) is applicable (see e.g. Fig. 1, the region at $c_t < 7.5$ mM).

Next, from a given sample of dried crystalline acid soap, we prepare a series of aqueous solutions and, at the working temperature, we measure their electrolytic conductivity, κ, as a function of the concentration, C, of the dissolved substance. The conductivity of the investigated 1:1 electrolyte solutions can be expressed in the form [26]:

$$\kappa = \kappa_0 + \lambda^{(0)} I + A I^{3/2}, \tag{3}$$

where

$$\lambda^{(0)} = \lambda_M^{(0)} + \lambda_Z^{(0)} \tag{4}$$

is the molar conductance of a MZ solution at infinite dilution; $\lambda_M^{(0)}$ and $\lambda_Z^{(0)}$ are the respective molar ionic conductances at infinite dilution; Eq. (4) expresses the Kohlrausch law [27]; κ_0 and A are experimental constants; κ_0 accounts for possible trace amounts of other ionic species (like H^+, OH^-, HCO_3^-) in the used water. In the ideal case, $\kappa_0 \approx 0$ and Eq. (3) reduces to the known expression [26]: $\kappa/I = \lambda^{(0)} + A I^{1/2}$.

As already mentioned, the working temperature is chosen in such a way that the dissolution of $(HZ)_j(MZ)_n$ acid soap yields M^+ cations, Z^- anions, and HZ crystallites. The concentration of the investigated solutions, C (g/L), can be expressed in the form

$$C \approx M_M c_M + M_Z c_Z + M_{HZ} m_{HZ}, \tag{5}$$

where M_M, M_Z and M_{HZ} (g/mol) are the molecular masses of the respective components; m_{HZ} is the concentration of HZ molecules

in the form of HZ precipitate per unit volume of the solution; the concentration of *molecularly* dissolved carboxylic acid, c_{HZ}, is very small and it is neglected; here, the dimension of c_Z, c_M, and m_{HZ} is mol/L. In view of the stoichiometry of the dissolved $(HZ)_j(MZ)_n$ acid soap, we have:

$$\frac{c_M}{m_{HZ}} = \frac{n}{j}, \quad \text{hence } m_{HZ} = \frac{j}{n}c_M. \tag{6}$$

With the help of Eqs. (2) and (6), we can represent Eq. (5) in the form:

$$I = \frac{C}{M_{MZ} + (j/n)M_{HZ}}, \tag{7}$$

where $M_{MZ} = M_M + M_Z$ is the molecular mass of the neutral soap.

The theoretical dependence $\kappa(C)$ is determined by Eqs. (3) and (7). For a given C, and for a tentative value of j/n, we calculate I from Eq. (7), and then the value of I is substituted in Eq. (3) to calculate κ. The molecular masses M_{MZ} and M_{HZ} are known. The parameters κ_0, $\lambda^{(0)}$ and A are determined in a separate experiment (see Section 3). The ratio j/n can be determined as a single adjustable parameter from the fit of the data for $\kappa(C)$; see Section 4.

3. Concentration dependence of the conductivity of carboxylate solutions

3.1. Theoretical background

As known, with the increase of the total carboxylate concentration, c_t, different kinds of solid precipitates (HZ and *j:n* acid soaps) and micelles appear in the aqueous carboxylate solutions [3,12–14,19–21]. The electrolytic conductivity of these solutions, κ, may exhibit one or more kinks when plotted as a function of c_t [21,22,28–30]. This is due to the fact that the appearance of micelles and/or acid soap precipitates of different stoichiometry affects the types and concentrations of the ionic species in the solution. In principle, the detailed analysis of the composition of the carboxylate solutions, like that in Refs. [4,21,22], could reveal the types of the precipitates/micelles and allow a quantitative interpretation of the data for κ vs c_t.

According to the theory by Onsager and Fuoss [31], the molar conductance of a binary solution can be expressed in the form [26,31]:

$$\lambda = \lambda^{(0)} - (A_1 + A_2)(2I)^{1/2}, \tag{8}$$

where

$$A_j = \frac{1.970 \times 10^6 |z_1 z_2| q \lambda_j^{(0)}}{(\varepsilon T)^{3/2}(1+q^{1/2})} + \frac{28.98|z_j|}{\eta(\varepsilon T)^{1/2}} \quad (j = 1, 2), \tag{9}$$

ε and η are the dielectric constant and viscosity (in poises) of the solvent; T is the absolute temperature; z_1 and z_2 are the valences of the cations and anions; $\lambda_1^{(0)}$ and $\lambda_2^{(0)}$ are their molar conductances at infinite dilution:

$$q = \frac{|z_1 z_2|(\lambda_1^{(0)} + \lambda_2^{(0)})}{(|z_1| + |z_2|)(|z_2|\lambda_1^{(0)} + |z_2|\lambda_2^{(0)})}. \tag{10}$$

For 1:1 electrolyte, we have $q = 0.5$. In addition, the ionic molar conductance can be expressed in the form [26]:

$$\lambda_j^{(0)} = \frac{z_j e^2 N_A}{6\pi\eta r_j}, \tag{11}$$

where e is the electronic charge, N_A is the Avogadro number, and r_j is the radius of the ion.

The first term in the right-hand side of Eq. (9) accounts for the *relaxation* effect; this term depends on the ionic radius, r_j, through $\lambda_j^{(0)}$. The last term in Eq. (9) accounts for the *electrophoretic* effect; this term is independent of the ionic radius, r_j, and is the same for different ions of the same valence.

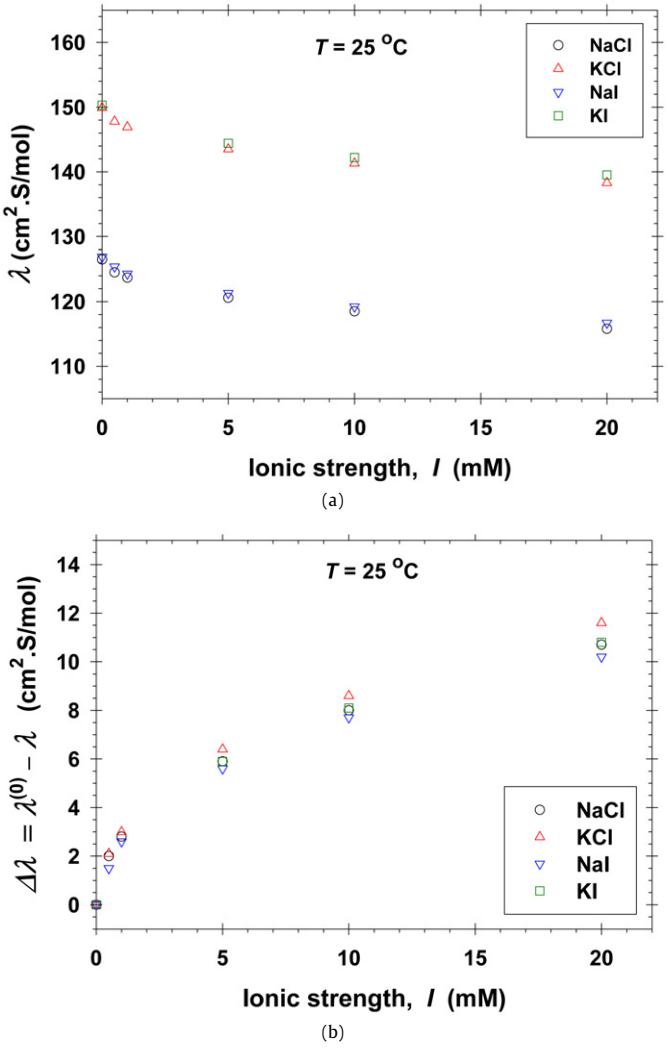

Fig. 2. (a) Molar conductance of solution of four electrolytes (NaCl, KCl, NaI, and KI) vs the solutions' ionic strength, I. (b) Plot of the correction term, $\Delta\lambda = \lambda^{(0)} - \lambda$, vs I for the same electrolytes. Plots of data from Refs. [26] and [32].

On the basis of a set of experimental data, Walden et al. [24,25] arrived at the following semiempirical equation:

$$\lambda = \lambda^{(0)} - AI^{1/2}, \quad A \approx \frac{65.7}{\varepsilon\eta}, \tag{12}$$

which was found to be applicable to a large number of electrolytes in different solvents [26]. Equation (12) implies that only $\lambda^{(0)}$ is sensitive to the type of the ion (through r_j—see Eq. (11)), whereas the parameter A in the correction term is the same for different 1:1 electrolytes [24–26].

To check the applicability of the Walden's approach, in Fig. 2 we have plotted literature data for λ from Refs. [26] and [32] for four electrolytes, NaCl, KCl, NaI, and KI, at 25 °C. On the one hand (Fig. 2a), there is a difference between some of the experimental curves, which are mostly due to the different $\lambda_j^{(0)}$ for the Na^+ and K^+ ions ($\lambda_{Na}^{(0)} = 50.1$ vs $\lambda_K^{(0)} = 73.5$ cm² S/mol; 25 °C). On the other hand, *the correction term*, $\Delta\lambda \equiv \lambda^{(0)} - \lambda$, is almost the same for these four different electrolytes (Fig. 2b). This result is agreement with the Walden's approach; see Eq. (12). In view of Eq. (9), this implies that the electrophoretic effect is predominant. [If the

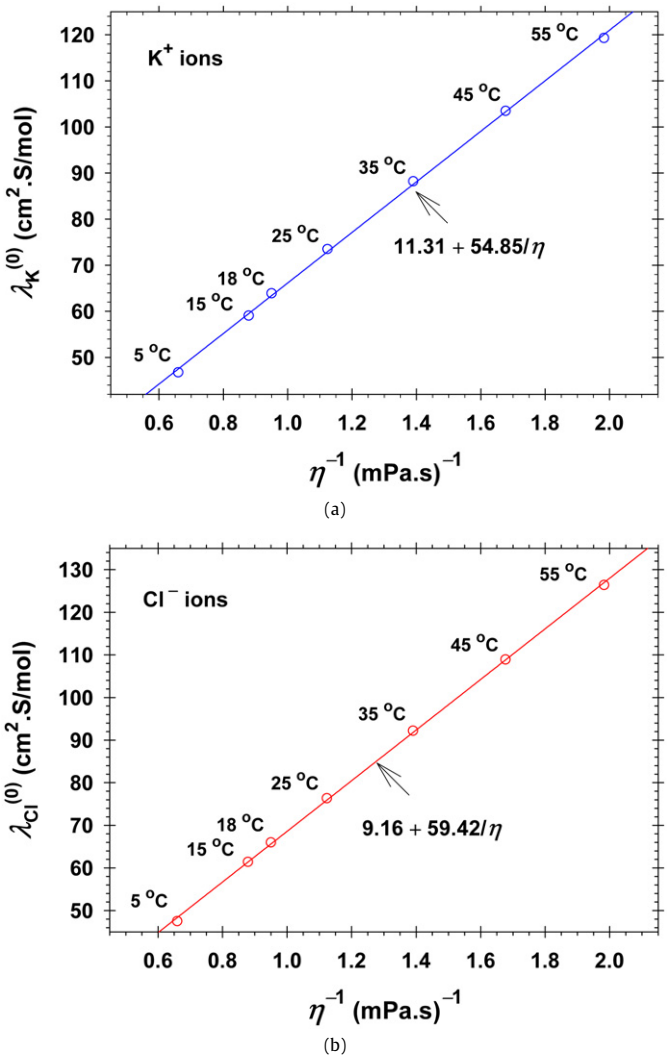

Fig. 3. Plots of the limiting molar ionic conductance of (a) K^+ and (b) Cl^- ions as functions of the inverse viscosity of water, η^{-1}. The lines are linear regressions.

relaxation effect were important, this would lead to influence of r_j on $\Delta\lambda$ through $\lambda_j^{(0)}$, see Eqs. (9) and (11), which is not the case.]

Following the Walden's approach, below we check whether the correction term, $\Delta\lambda \equiv \lambda^{(0)} - \lambda$, is the same for KCl and KMy. If this is confirmed, we may use $\Delta\lambda$, obtained from the available accurate set of data for the conductivity of KCl, to interpret the conductivity data for solutions of KMy and its acid soaps.

3.2. Temperature dependence of $\lambda^{(0)}$

To analyze our data, we need the values of $\lambda_j^{(0)}$ for K^+ and Cl^- ions at 40 °C. For this goal, we used literature data for $\lambda_j^{(0)}(T)$ from Ref. [33], which were interpolated to determine the value at 40 °C, see Fig. 3. The same interpolation curves might be used to obtain the value of $\lambda_j^{(0)}$ at other temperatures. We utilized the fact that the main temperature dependence of $\lambda_j^{(0)}$ originates from the strong dependence of the viscosity of water, η, on temperature. For this reason, in Fig. 3 we plot $\lambda_j^{(0)}$ vs η^{-1}, which turns out to be a straight line:

$$\lambda_X^{(0)} = a_X + \frac{b_X}{\eta} \tag{13}$$

Table 1
Molar ionic conductances, $\lambda_j^{(0)}$ (cm^2 S/mol), of several ions in aqueous solutions at infinite dilution, and at three different temperatures

Conductance	10 °C	25 °C	40 °C
$\lambda_{Na}^{(0)}$	34.88	50.10	67.56
$\lambda_{K}^{(0)}$	52.96	73.50	95.69
$\lambda_{Cl}^{(0)}$	54.32	76.35	100.6
$\lambda_{H}^{(0)}$	275.4	349.8	419.1
$\lambda_{OH}^{(0)}$	141.4	198.3	260.6
$\lambda_{HCO_3}^{(0)}$	30.34	44.50	60.66
$\frac{1}{2}\lambda_{CO_3}^{(0)}$	47.24	69.30	94.47

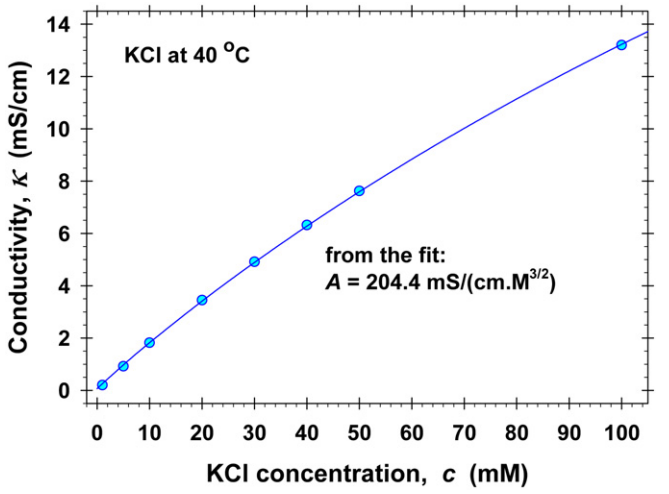

Fig. 4. Plot of experimental data for the conductivity, κ, of KCl solutions vs the KCl concentration, c. The line is the best fit by Eq. (14).

(X = K, Cl, ...). The coefficients a_X and b_X, determined from the interpolating linear regression, are given in Fig. 3. Similar approach is applicable also to other ions. For example, for Na^+ ions, Eq. (13) is applicable with $a_X = 2.19$ and $b_X = 42.70$ (the same units as in Fig. 3). As an illustration of the temperature effect, results that are useful for the analysis of conductivity of carboxylate solutions are shown in Table 1 for several ions at three different temperatures: 10, 25 and 40 °C.

3.3. Comparison of the conductivities of KMy and KCl at 40 °C

In this case, the conductivity of the investigated solutions can be described by the expression:

$$\kappa = \kappa_0 + \lambda^{(0)} c - A c^{3/2} \quad (T = 40\,^\circ\mathrm{C}), \tag{14}$$

where $c = I$ is the concentration of the 1:1 electrolyte solution; κ_0 is the same as in Eq. (3).

Fig. 4 shows our experimental data for the conductivity $\kappa(c)$ of KCl at 40 °C. For this system, the coefficient $\lambda^{(0)}$ in Eq. (14) is known: from Table 1 we find $\lambda^{(0)} = \lambda_K^{(0)} + \lambda_{Cl}^{(0)} = 196.29$ cm^2 S/mol. Using the latter value, we fitted the data in Fig. 4 by means of Eq. (14), and determined κ_0 and A as adjustable parameters. Thus, we obtained: $\kappa_0 = 0.064 \pm 0.02$ mS cm^{-1}, $A = 204.4 \pm 1.5$ mS cm^{-1} $M^{-3/2}$.

In addition, we obtained data for the conductivity of KMy solutions at 40 °C and at concentrations $c < 7.5$ mM (below the CMC). Under these conditions, the solutions contain K^+ and Z^- ions, and HZ precipitate. To process the conductivity data for KMy, we will apply Eq. (14). Following the Walden's approach we will use *the*

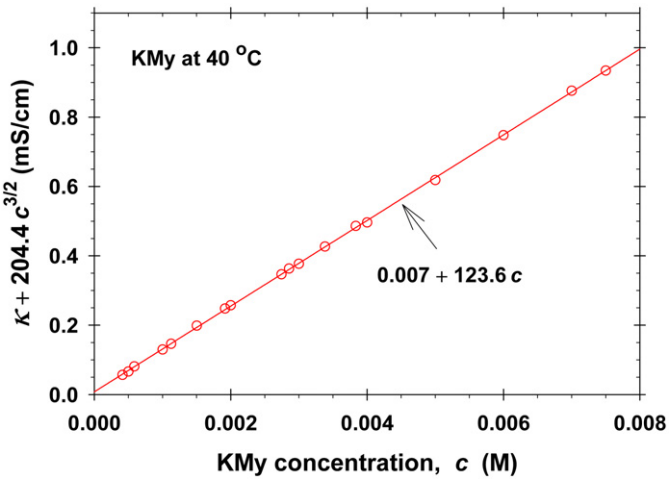

Fig. 5. Plot of experimental data for the conductivity, κ, of KMy solutions vs the KMy concentration, c, in accordance with Eq. (15). The line is the best fit by linear regression.

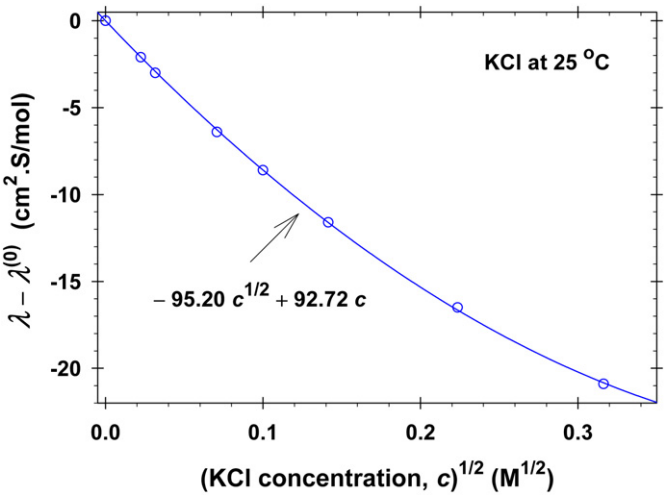

Fig. 6. Plot of the molar ionic conductance of KCl solutions vs $c^{1/2}$ in accordance with Eq. (18); data from Refs. [26] and [32]. The parameters of the best fit are shown in the figure.

same value of A as for KCl. In such a case, Eq. (14) can be represented in the form:

$$\kappa + 204.4c^{3/2} = \kappa_0 + \lambda^{(0)}c. \tag{15}$$

The data for the conductivity $\kappa(c)$ of KMy solutions at 40 °C are plotted in Fig. 5 in accordance with Eq. (15). The fit by linear regression has intercept $\kappa_0 = 0.007 \pm 0.003$ mS/cm; slope $\lambda^{(0)} = 123.6 \pm 0.8$ cm^2 S/mol, and regression coefficient = 0.99994. The latter coefficient indicates that the data in Fig. 5 excellently comply with a straight line, which means that the Walden's approach is applicable, i.e. the same value of A can be used for KCl and KMy.

Furthermore, with the above value of $\lambda^{(0)}$, and with $\lambda_K^{(0)}$ from Table 1, we determine the molar conductance of the My^- ion:

$$\lambda_{My}^{(0)} = \lambda^{(0)} - \lambda_K^{(0)} = 27.9 \text{ cm}^2 \text{ S/mol at } 40\,^\circ\text{C}. \tag{16}$$

Additional results presented in Section 3.4 will confirm that the latter value of $\lambda_{My}^{(0)}$ is reasonable.

In summary, in the present section, we determined the values of the coefficients in Eq. (3) for KMy at 40 °C, as follows:

$$\kappa = 0.007 + 123.6I - 204.4I^{3/2} \quad (T = 40\,^\circ\text{C}) \tag{17}$$

($I = c$ for 1:1 electrolyte). Equation (17) will be applied in Section 4 for determination of the stoichiometry of acid soaps.

3.4. Comparison of the conductivities of KMy and KCl at 25 °C

To confirm the correctness of the above approach, and of the obtained value of $\lambda_{My}^{(0)}$, we will process in a similar way data for the conductivity of KCl and KMy solutions at 25 °C. Unlike the case at 40 °C, an expression in the form $\lambda = \lambda^{(0)} - Ac^{1/2}$ is insufficient to describe the concentration dependence of the molar conductance of KCl at 25 °C, in the concentration range $c \leqslant 150$ mM. For this purpose, an augmented expression for λ can be used [26]:

$$\lambda = \lambda^{(0)} - Ac^{1/2} + Bc \quad (T = 25\,^\circ\text{C}). \tag{18}$$

For KCl at 25 °C, we have $\lambda^{(0)} = 149.85$ cm^2 S/mol. We determined the coefficients A and B by fit of literature data [26,32] for λ of KCl, see Fig. 6. The best fit in the latter figure yields: $A = 95.20 \pm 0.72$ mS cm^{-1} M$^{-3/2}$, $B = 92.72 \pm 2.7$ mS cm^{-1} M^{-2}; the regression coefficient is 0.99993. Note that the last term, Bc, is negligible for $c \leqslant 15$ mM.

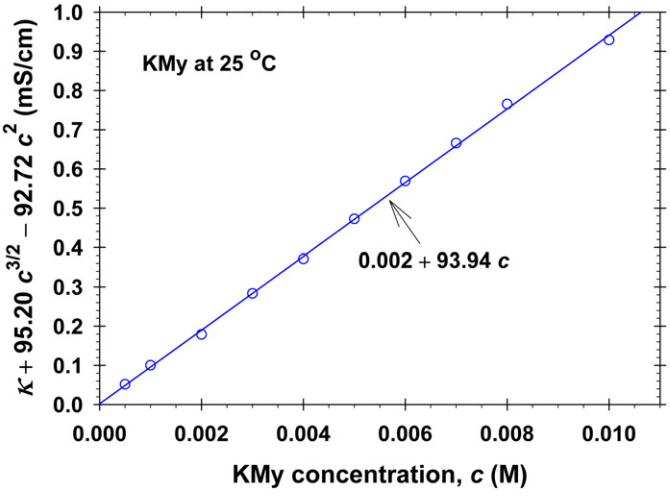

Fig. 7. Plot of experimental data for the conductivity, κ, of KMy solutions vs the KMy concentration, c, in accordance with Eq. (20). The line is the best fit by linear regression.

Furthermore, we obtained conductivity data for KMy at 25 °C for concentrations below the CMC. To fit these data, we used the expression

$$\kappa = \kappa_0 + \lambda^{(0)}c - Ac^{3/2} + Bc^2 \quad (T = 25\,^\circ\text{C}), \tag{19}$$

which is an upgraded version of Eq. (14), in view of Eq. (18). Following the Walden's approach, we assumed that the correction term, $-Ac^{3/2} + Bc^2$, is the same for KCl and KMy, and processed the data for KMy by means of the expression:

$$\kappa + 95.20c^{3/2} - 92.72c^2 = \kappa_0 + \lambda^{(0)}c \quad (T = 25\,^\circ\text{C}). \tag{20}$$

The data for the conductivity $\kappa(c)$ of KMy solutions at 25 °C are plotted in Fig. 7 in accordance with Eq. (20). The fit by linear regression has intercept $\kappa_0 = 0.002 \pm 0.004$ mS/cm; slope $\lambda^{(0)} = 93.94 \pm 0.8$ cm^2 S/mol, and regression coefficient = 0.9997. The latter coefficient indicates that the data in Fig. 7 excellently comply with a straight line, which means that the Walden's approach is applicable again.

Furthermore, with the above value of $\lambda^{(0)}$, and with $\lambda_K^{(0)}$ from Table 1, we determine the molar conductance of the My^- ion:

$$\lambda_{My}^{(0)} = \lambda^{(0)} - \lambda_K^{(0)} = 20.44 \text{ cm}^2 \text{ S/mol at } 25\,^\circ\text{C}. \tag{21}$$

On the other hand, using Eq. (16) we calculate

$$\lambda^{(0)}_{\mathrm{My}}(25\,^\circ\mathrm{C}) \approx \frac{\eta(40\,^\circ\mathrm{C})}{\eta(25\,^\circ\mathrm{C})}\lambda^{(0)}_{\mathrm{My}}(40\,^\circ\mathrm{C}) = 20.5\ \mathrm{cm^2\,S/mol}, \tag{22}$$

where the intercept a_X in Eq. (13) has been neglected, and the respective values of the viscosity of water have been substituted: $\eta\ (25\,^\circ\mathrm{C}) = 0.8903$ and $\eta\ (40\,^\circ\mathrm{C}) = 0.6531$ (mPa s). The values of $\lambda^{(0)}_{\mathrm{My}}$ in Eqs. (21) and (22) agree very well, which confirms the applicability of the used approach.

In summary, in the present section, we determined the coefficients in the concentration dependence of conductivity for KMy at 25 °C:

$$\kappa = 0.002 + 93.94I - 95.20I^{3/2} + 92.72I^2 \quad (T = 25\,^\circ\mathrm{C}), \tag{23}$$

which is used for interpretation of our data for the conductivity of KMy solutions in Ref. [22].

4. Determination of the acid-soap stoichiometry

4.1. Experimental procedure

Solutions of potassium myristate (KMy) were prepared by using two different procedures.

Procedure 1: KMy solutions were obtained by dissolving stoichiometric amounts of myristic acid (HMy, Fluka, 98% pure) and potassium hydroxide (KOH, Teokom, pure for analysis) at 60 °C, and stirring for 30 min. Then, the solutions were cooled down to 25 °C.

Procedure 2: The same as Procedure 1, but commercial KMy (producer Viva Corporation) was dissolved.

In some experiments (Procedure 1), the amount of KOH was 87.5% of that needed for full neutralization of HMy. The obtained solutions contain 87.5% KMy and 12.5% HMy. Thus, we checked the effect of added HMy on the precipitates in the investigated solutions. In other experiments, KCl (product of Sigma) was added to the solutions.

In many of the investigated solutions, we observe the formation of crystallites of size greater than 1 μm, which can be seen by optical microscopy. To separate these crystallites from the solution, the latter was poured in a filtration module, with a porous glass filter S3 at the bottom. In our experiments, we used a glass membrane of maximum pore size 33 μm. The aqueous phase is sucked out from the filtration module by a water pump for about 5–10 min depending on the volume of the filtrated solution. The crystallites are deposited at the upper surface of the glass filter. After that, they are placed in a Petri dish and dried in a vacuum drier at room temperature.

The working solutions for conductivity analysis were prepared by dissolving corresponding amounts of the collected crystallites at 60 °C to obtain a solution of a given concentration, C g/L. Finally, the solutions were cooled down to the working temperature of 40 °C, and their electrolytic conductivity, κ, was measured. In our first set of κ-measurements, we maintained $40 \pm 2\,^\circ$C, which led to some scattering of the data. Further, we improved the temperature control and succeeded to maintain $40 \pm 0.1\,^\circ$C, which resulted in smoother experimental curves.

4.2. Experimental results and their interpretation

Fig. 8a shows κ-vs-C experimental data for dissolved acid-soap crystallites that have been initially formed in a solution of 8.5 mM KMy at 25 °C, prepared by Procedure 1. This concentration is just above the CMC, which is 7.5 mM KMy for this system [22]. During the conductivity analysis, the temperature was maintained $40 \pm 0.1\,^\circ$C for the points denoted by circles, and $40 \pm 2\,^\circ$C for the points denoted by triangles. The theoretical line is drawn by means of Eqs. (7) and (17) for $j/n = 1$. The fact that this theoretical line complies very well with the experimental data indicates that the investigated crystallites are of 1:1 acid soap.

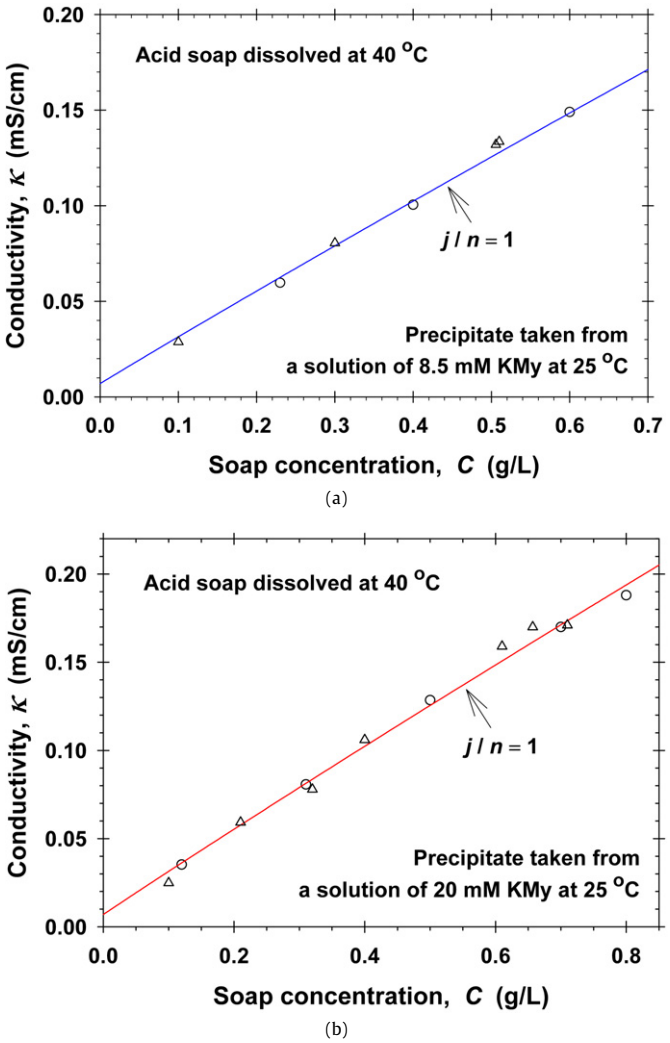

Fig. 8. κ-vs-C plot of experimental data for dissolved acid-soap crystallites that have been initially formed in (a) solution of 8.5 mM KMy at 25 °C, prepared by Procedure 1, and (b) solution of 20 mM KMy at 25 °C, prepared by Procedure 2. The temperature is maintained $40 \pm 0.1\,^\circ$C and $\pm 2\,^\circ$C, respectively, for the points denoted by circles and triangles. The theoretical lines are drawn by means of Eqs. (7) and (17) for $j/n = 1$.

Fig. 8b shows κ-vs-C experimental data for dissolved acid-soap crystallites that have been initially formed in a solution of 20 mM KMy at 25 °C, prepared by Procedure 2. This concentration corresponds to about 3 times the CMC. During the conductivity analysis, the temperature was maintained $40 \pm 0.1\,^\circ$C for the points denoted by circles, and $40 \pm 2\,^\circ$C for the points denoted by triangles. The theoretical line is drawn by means of Eqs. (7) and (17) for $j/n = 1$. Again, the theoretical line agrees very well with the experimental data indicating that the investigated crystallites are of 1:1 acid soap.

Fig. 9a shows κ-vs-C experimental data for dissolved acid-soap crystallites that have been initially formed in a 100 mM solution of 87.5% KMy and 12.5% HMy at 25 °C (without added KCl), prepared by Procedure 1. This concentration is 10 times the CMC, which corresponds to a total surfactant concentration of 10 mM for this system [22]. During the conductivity analysis, the temperature was maintained $40 \pm 0.1\,^\circ$C. The theoretical line, which is drawn by means of Eqs. (7) and (17) for $j/n = 1$, complies very well with the experimental data indicating that the investigated crystallites are of 1:1 acid soap, again.

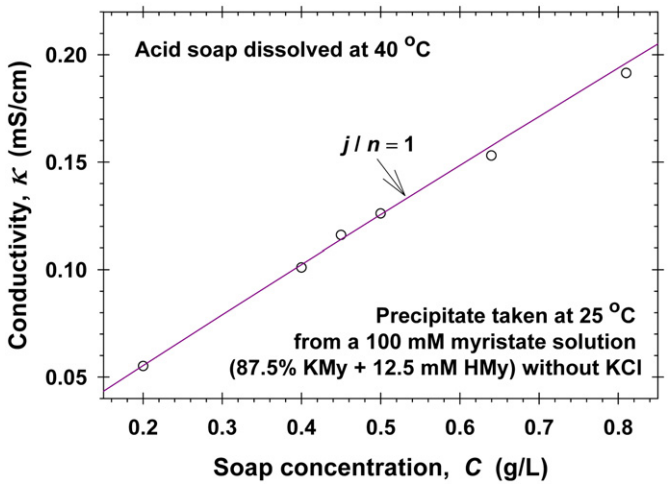

(a)

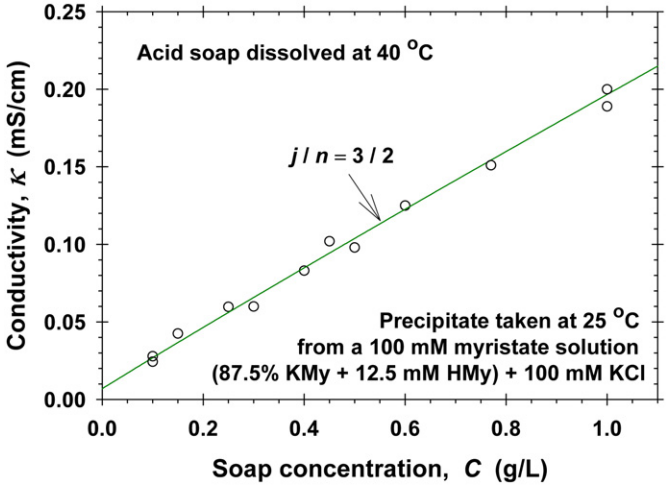

(b)

Fig. 9. κ-vs-C plot of experimental data for dissolved acid-soap crystallites that have been initially formed in 100 mM solutions of 87.5% KMy and 12.5% HMy at 25 °C, prepared by Procedure 1: (a) Without added KCl at $T = 40 \pm 0.1$ °C; the fit is drawn for $j/n = 1$. (b) With added 100 mM KCl at $T = 40 \pm 2$ °C; the fit is drawn for $j/n = 3/2$. In both cases, Eqs. (7) and (17) have been used to fit the data.

Fig. 9b shows κ-vs-C experimental data for dissolved acid-soap crystallites that have been initially formed in a 100 mM solution of 87.5% KMy and 12.5% HMy + 100 mM KCl at 25 °C, prepared by Procedure 1. This concentration is 50 times the CMC, which corresponds to a total surfactant concentration of 2 mM for this system [22]. During the conductivity analysis, the temperature was maintained 40 ± 2 °C. The theoretical line is drawn by means of Eqs. (7) and (17) for $j/n = 3/2$. The fact that this theoretical line agrees very well with the experimental data indicates that the investigated crystallites are of 3:2 acid soap.

In Fig. 10, we compare the κ-vs-C experimental data and theoretical curves obtained for different samples of soap crystallites. The upper curve (A) represents a part of the results for KMy shown in Fig. 5. The symbols denoted by B, C, and D are the data from Figs. 8a, 8b, and 9a. The diamond symbols denoted by E correspond to the data in Fig. 9b. The symbols denoted by F and G are data for crystallites taken, respectively, from 4 and 150 mM KMy solutions at 25 °C; the fit shows that both of them are of 1:1 acid soap.

The comparison of the results in Fig. 10 indicates that the proposed conductivity method for analysis of acid soaps is sensitive enough to distinguish between soaps of different stoichiometry

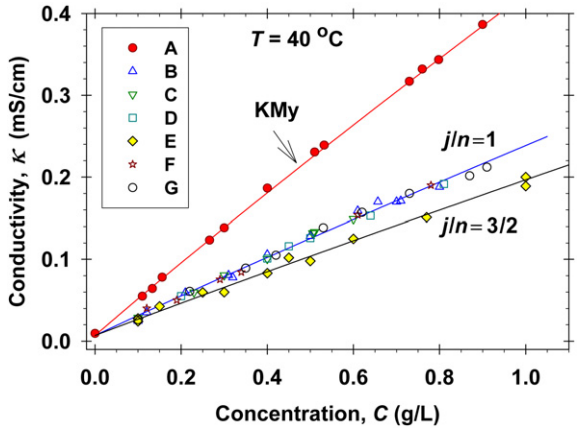

Fig. 10. Comparison of κ-vs-C plots of experimental data and theoretical curves obtained for different samples of soap crystallites. The upper curve (A) represents a part of the results for KMy shown in Fig. 5. The other curves are obtained by dissolving (at 40 °C) crystallites that have been collected at 25 °C from the following aqueous solutions: B—8.5 mM KMy (Fig. 8a); C—20 mM KMy (Fig. 8b); D—100 mM solution of 87.5% KMy and 12.5% HMy (Fig. 9a); E—100 mM solution of 87.5% KMy and 12.5% HMy + 100 mM KCl (Fig. 9b); F—4 mM KMy; G—150 mM KMy.

supposedly the working temperature during the conductivity measurements (40 °C in the present study) is maintained with a sufficient accuracy.

4.3. Discussion

A new step in the present article is that the conductivity is used as a *quantitative* method for analysis of carboxylate solutions. In the previous papers on this theme [21,28–30], only the kinks in the conductivity curves were used as indicators for the appearance of micelles or changes in the stoichiometry of the acid-soap precipitates. This is related to the known fact that the popular theoretical expression by Onsager and Fuoss, Eqs. (8)–(9), is not quantitative, i.e. it does not agree well with the experiment. Here, we combined an empirical (but quantitative) expression for conductivity, Eq. (3) or Eq. (19), with the Walden's finding [24,25] that the correction term, and in particular the coefficients A and B (unlike $\lambda^{(0)}$) are not sensitive to the ionic size. We first determined A and B for KCl (Figs. 4 and 6), and the results were further applied to KMy solutions to determine $\lambda^{(0)}_{\mathrm{My}}$ at the respective temperature (Figs. 5 and 7). In this way, we find all coefficients in Eq. (3) or Eq. (19), which in combination with Eq. (7) gives the theoretical dependence $\kappa(C)$. The latter contains a single adjustable parameter, the acid-soap stoichiometry, j/n, which is finally determined from the fit of the experimental data for κ; see Figs. 8–10.

From the viewpoint of future applications, it should be noted that the values of the coefficients A and B can be found in some handbooks [34] for many electrolytes at some temperatures. Alternatively, we could experimentally determine A and B at the working temperature, as this is done in the present study.

One limitation of the proposed method is that it is not applicable when the ratio j/n is very small. Indeed, the term $(j/n)M_{\mathrm{HZ}}$ in Eq. (7) must not be negligible in comparison with M_{MZ}. Otherwise, the solution's ionic strength and conductivity will be insensitive to the stoichiometry of the dissolved acid soap.

The second limitation of this method, and of all methods that are based on the use of samples of dried acid- or neutral-soap crystals, is that in some cases the amount of crystallites in the solution is very small, or their size is very small (smaller than 1 μm), so that it is very difficult to prepare samples of dried crystals. In the latter case, one could use the *in situ* method [4,21,22], which is based on pH measurements directly in the mother solutions, without the necessity to separate and dry crystallites; see Section 5.

5. Confirmation of the results by independent pH measurements

5.1. Theoretical background

In the case when a precipitate of carboxylic acid (HZ) crystallites is present in the solution, the respective chemical equilibrium relation reads [4,21]:

$$c_H c_Z \gamma_\pm^2 = K_{HZ}, \tag{24}$$

where c_H and c_Z are the concentrations of the respective ions in the solution; $K_{HZ} = \text{const.}$ is the solubility product of HZ; $\gamma_\pm$ is the activity coefficient tabulated in [33]. The combination of Eq. (24) with the electroneutrality condition and other chemical-equilibrium relationships leads to the expression [4,21]:

$$(c_t + c_H) c_H \gamma_\pm^2 = K_t = \text{const.} \tag{25}$$

The total input concentration of carboxylate (in our case KMy) is known, and c_H is determined by pH measurements [$\text{pH} \equiv -\log(c_H\gamma_\pm)$]. Equation (25) can be compared with the experimental data in two different ways.

First, as suggested by Lucassen [4] for $c_H \ll c_t$ and $\gamma_\pm \approx 1$, Eq. (25) can be represented in the form:

$$\text{pH} \approx \log c_t - \log K_t, \tag{26}$$

i.e. the slope of the pH vs log c_t plot is +1 if a HZ precipitate is present [4]; see Fig. 11a.

Second, taking log of Eq. (25) we define the characteristic function for precipitate of carboxylic acid [21]:

$$f_{HZ} \equiv \log\left[(c_t + c_H) c_H \gamma_\pm^2\right] = \log K_t = \text{const.} \tag{27}$$

The concentration region, in which HZ precipitate is present, is identified in the following way. The function f_{HZ}, defined by Eq. (27), is plotted vs c_t using the experimental $c_H(c_t)$ dependence (determined by pH measurements). In the concentration region where a precipitate of HZ is present, the curve $f_{HZ}(c_t)$ exhibits a plateau, whose height is equal to $\log K_t$; see Fig. 11b.

In the case when a precipitate of j:n acid soap, $(HZ)_j(MZ)_n$, is present in the solution, the respective chemical equilibrium relation reads [21]:

$$c_H^j c_M^n c_Z^{j+n} \gamma_\pm^{2j+2n} = K_{jn} \quad (j, n = 1, 2, 3, \ldots), \tag{28}$$

where $K_{jn} = \text{const.}$ is the solubility product for the j:n acid-soap crystallites. Under typical experimental conditions, we have $c_Z \approx c_t$ and $c_M \approx c_t + c_A$ [21], where c_A is the concentration of the added inorganic electrolyte (in our case KCl), and then Eq. (28) acquires the form:

$$c_H^j (c_t + c_A)^n c_t^{j+n} \gamma_\pm^{2j+2n} \approx K_{jn} = \text{const.} \tag{29}$$

Equation (29) can be compared with the experimental data in the following two ways.

First, for $\gamma_\pm \approx 1$ and $c_A = 0$, Eq. (29) can be represented in the form [21]:

$$\text{pH} \approx (1 + 2n/j)\log c_t - (1/j)\log K_{jn}, \tag{30}$$

i.e. the slope of the pH vs log c_t plot is equal to $(1 + 2n/j)$ if a j:n acid-soap precipitate is present; see e.g. Fig. 11a, where $(1 + 2n/j) = 3$ for 1:1 acid-soap precipitate.

Second, taking log of Eq. (29) we define the characteristic function for precipitate of j:n acid soap [21]:

$$f_{jn} \approx \log\left[(c_t + c_A)^n c_t^{j+n} \gamma_\pm^{2j+2n}\right] - j\text{pH}, \tag{31}$$

$j, n = 1, 2, 3, \ldots$. The concentration region, in which j:n acid-soap precipitate is present, is identified in the following way. The function f_{jn}, defined by Eq. (31), is plotted vs c_t using the experimental $c_H(c_t)$ dependence (determined by pH measurements). In the concentration region where a precipitate of j:n acid soap is present, the curve $f_{jn}(c_t)$ exhibits a plateau, whose height is equal to $\log K_{jn}$. We have to check for which values of j and n the characteristic function f_{jn} exhibits a horizontal plateau. In Fig. 11b, this is the case of $j = n = 1$, i.e. the precipitate is of 1:1 acid soap.

5.2. Solutions of KMy at 25 °C

Fig. 11a shows of experimental data for pH vs c_t measured for KMy solutions at 25 °C. In the concentration region $0.008 < c_t < 1.6$ (mM) the data comply with a straight line of slope +1, which indicates that the precipitate in these solutions is of HZ; see Eq. (26). This is confirmed by the plateau of the function $f_{HZ}(c_t)$ in Fig. 11b.

Further, in the concentration region $1.6 < c_t < 10$ (mM) the data in Fig. 11a comply with a straight line of slope +3, which indicates that the precipitate in these solutions is of 1:1 acid soap; see Eq. (30). This is also confirmed by the plateau of the function $f_{11}(c_t)$ in Fig. 11b. Because the concentrations 4 and 8.5 mM, at which crystallites have been taken from a KMy solution at 25 °C, belongs to the interval $1.6 < c_t < 10$ (mM), these crystallites are of 1:1 acid soap, which is in agreement with the result of the independent conductivity method proposed in the present article; see Fig. 8a, Fig. 10—curve F, and the related text.

The results in Fig. 11a indicate also that in the region $1.6 < c_t < 10$ (mM) the precipitate cannot be a mixture of acid soaps. This is guaranteed by the Gibbs phase rule. Indeed, if a second kind of acid-soap crystals (of different stoichiometry) were present, the pH would be constant as it follows from the Gibbs phase rule [4], which is not fulfilled in this concentration region.

In Fig. 11a, pH is constant for $c_t > 10$ mM. In addition, Fig. 11c shows that the conductivity of these solutions exhibits a kink at $c_t = 10$ mM. At $c_t > 10$ mM the conductivity increases, but with a smaller slope (as compared to the slope at $c_t < 10$ mM). Such a behavior of conductivity indicates the formation of micelles in these solutions for $c_t > 10$ mM. This is confirmed by independent oil-solubilization and film-stratification experiments in Ref. [22]. At 25 °C and $c_t > 10$ mM, the KMy solutions contain also microcrystalline precipitates, which are seen by direct microscopic observations. We collected such crystallites (from solutions of 20 and 150 mM KMy, see Fig. 8b and Fig. 10—curve G) as explained in Section 4.1, and subjected them to conductivity analysis at 40 °C. The results (like those in Fig. 10—curves C and G) show that the precipitate above the CMC is of 1:1 acid soap, at least in the investigated range, $10 < c_t < 150$ mM, i.e. the micelles appear on the background of the 1:1 acid soap crystallites, which are also present in the solutions in the neighboring concentration region below the CMC, $1.6 < c_t < 10$ mM; see above. In other words, the appearance of micelles does not change the stoichiometry of the acid-soap crystallites. In Ref. [22], this conclusion is confirmed by independent theoretical analysis from the value pH = 10.67 (Fig. 11a) and from the slope of the κ vs c_t dependence (Fig. 11c) at $c_t > 10$ mM.

It is worthwhile noting that the lack of a second kink of the κ vs c_t dependence in the region $10 < c_t < 150$ mM (Fig. 11c) indicates that there is no appearance of liquid-crystalline phases or other changes in the type of precipitate in this concentration region.

5.3. Solutions of 87.5% KMy and 12.5% HMy + 100 mM KCl at 25 °C

We chose to analyze this type of solutions, because the conductivity analysis (Fig. 9b) shows that they contain acid soap of different stoichiometry, viz. 3:2 acid soap.

Fig. 12a shows of experimental data for pH vs c_t measured at 25 °C for solutions that contain 87.5% KMy and 12.5% HMy + 100 mM KCl. For $c_t < 0.4$ (mM) the data comply with a straight

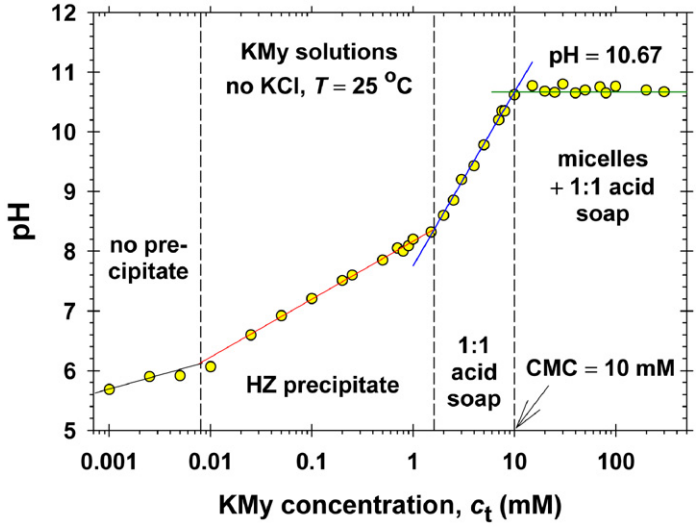

(a)

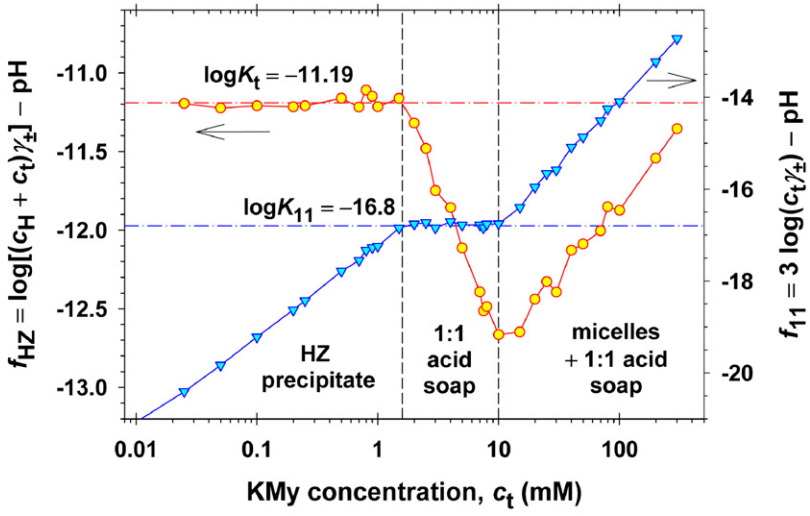

(b)

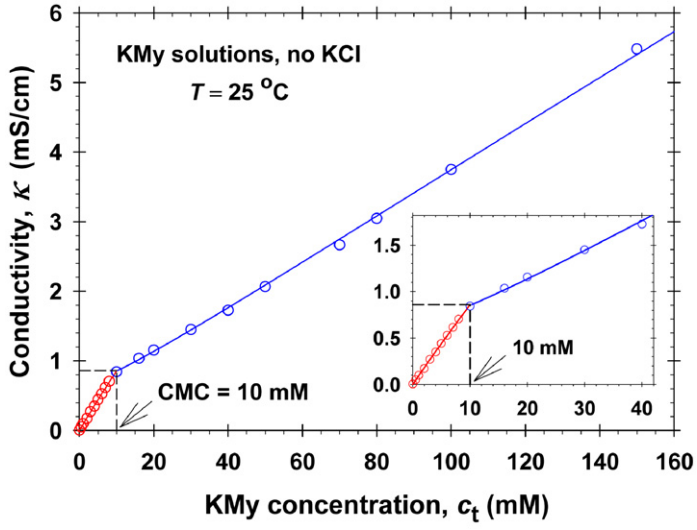

(c)

Fig. 11. Data for solutions of KMy at 25 °C. (a) Experimental data for pH vs c_t; the vertical dashed lines show the boundaries between zones with different precipitates. (b) Plots of the characteristic functions $f_{HZ}(c_t)$ and $f_{11}(c_t)$ calculated from Eqs. (27) and (31) using the experimental pH(c_t) dependence. (c) Experimental data for $\kappa(c_t)$ for $c_t \leqslant 150$ mM.

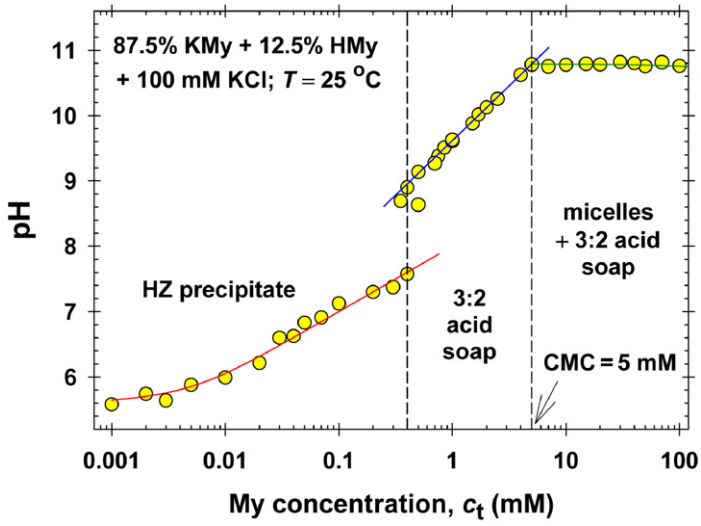

(a)

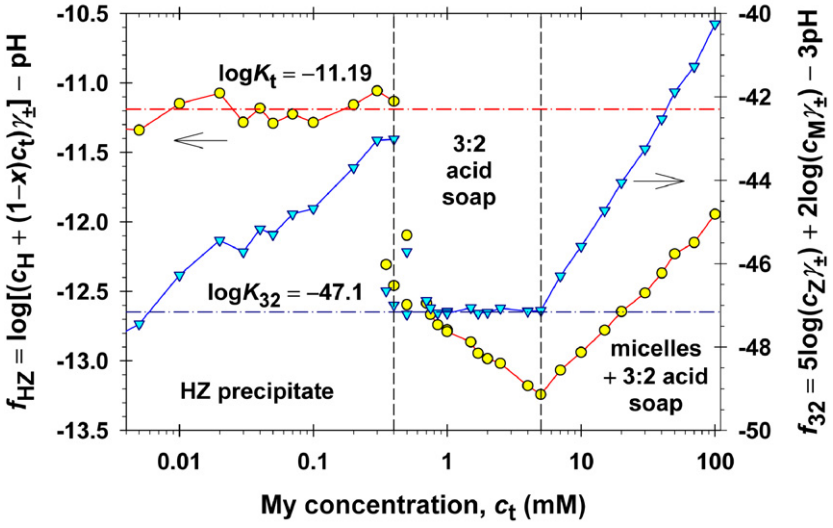

(b)

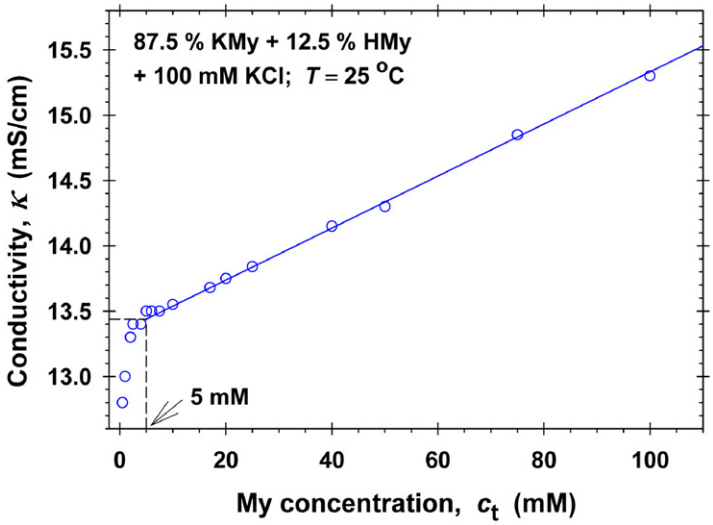

(c)

Fig. 12. Data for solutions of 87.5% KMy and 12.5% HMy + 100 nM KCl at 25 °C. (a) pH vs c_t; the vertical dashed lines are boundaries between zones with different precipitates. (b) The characteristic functions $f_{HZ}(c_t)$ and $f_{32}(c_t)$ calculated from Eqs. (27) and (31) using the experimental pH(c_t) dependence. (c) Experimental data for $\kappa(c_t)$ for $c_t \leqslant 110$ mM. c_t is the total input concentration of myristate due to both KMy and HMy; $x = 0.125$ is the molar fraction of HMy.

Table 2
Comparison of the values of j:n determined by the conductivity method (Section 4) and by the *in situ* pH method (Section 5 and Ref. [22])

Mother solution (25 °C)	j:n Section 4	j:n Section 5 and Ref. [22]
4 mM KMy	1:1	1:1
8.5 mM KMy	1:1	1:1
20 mM KMy	1:1	1:1
150 mM KMy	1:1	1:1
100 mM (87.5% KMy + 12.5% HMy)	1:1	1:1
100 mM (87.5% KMy + 12.5% HMy) + 100 mM KCl	3:2	3:2

line of slope +1, which indicates that the precipitate in these solutions is of HZ; see Eq. (26). This is confirmed by the plateau of the function $f_{HZ}(c_t)$ in Fig. 12b.

Further, in the concentration region $0.4 < c_t < 5$ (mM) the pH(c_t) data in Fig. 12a exhibits a linear dependence of a greater slope. In this case, Eq. (30) is not applicable, because $c_A = 100$ mM KCl, and $\gamma_\pm$ is essentially smaller than 1. However, the method based on Eq. (31) works and gives that the crystalline precipitates in these solutions are of 3:2 acid soap ($j = 3$, $n = 2$), see Fig. 12b. As seen in Figs. 12a and 12b, the transition from HZ to 3:2 acid-soap precipitates causes a considerable jump in the pH.

We see that in Fig. 12a we have pH ≈ constant for $c_t > 5$ mM. In addition, Fig. 12c shows that the conductivity of these solutions exhibits a kink at $c_t = 5$ mM. At $c_t > 5$ mM the conductivity increases, but with a smaller slope (as compared to the slope at $c_t < 5$ mM). As in Fig. 11c, such behavior of conductivity indicates the formation of micelles in the respective solutions (at $c_t > 5$ mM). This is confirmed by independent oil-solubilization and film-stratification experiments in Ref. [22]. At 25 °C and $c_t > 5$ mM, the investigated solutions contain also micro-crystalline precipitates. We collected such crystallites from solutions of 100 mM myristate (87.5% KMy + 12.5% HMy) as explained in Section 4.1, and subjected them to conductivity analysis at 40 °C. The results (Fig. 9b) show that the precipitate above the CMC (5 mM) is of 3:2 acid soap, i.e. the micelles appear on the background of the 3:2 acid soap crystallites, which are also present in the solutions in the neighboring concentration region below the CMC, $0.4 < c_t < 5$ mM; see above. In other words, the appearance of micelles does not change the stoichiometry of the acid-soap crystallites in these solutions. In Ref. [22], this conclusion is confirmed by independent theoretical analysis from the values of pH (Fig. 12a) and the slope of the κ vs c_t dependence (Fig. 12c) at $c_t > 5$ mM.

It should be also noted that the lack of a second kink of the κ vs c_t dependence in the region $5 < c_t < 110$ mM (Fig. 12c) indicates that there is no appearance of liquid-crystalline phases or other changes in the type of precipitate in this concentration region.

We compared the conductivity method from Section 4 with the pH method from Section 5 also for several other solutions. The results are summarized in Table 2. We see that in all investigated cases the two methods give coinciding results for the stoichiometry of the acid soaps.

6. Summary and conclusions

A method for determining the stoichiometry of acid soap crystallites is developed, which is based on electrolytic conductivity measurements. It is applied to aqueous solutions of potassium myristate (KMy), for which the working temperature is chosen to be 40 °C. At this temperature, the only precipitate is that of HZ for concentrations below the CMC (Fig. 1). In the theoretical model data interpretation, we took into account the dependence of the molar conductance on the electrolyte concentration by using the Walden's approach, which is semiempirical, but quantitative (Section 3). The fits of the data were drawn by means of Eqs. (7) and (17). The method was applied to determine the composition of six different samples of acid-soap crystallites (Figs. 8–10). The method is sensitive enough to distinguish between acid soaps of different composition (Fig. 10). The stoichiometry of all samples obtained in the present study coincides with that independently determined by pH measurements in the mother solutions (from which the crystallites have been collected); see Section 5, Table 2, and Ref. [22].

Acknowledgments

We gratefully acknowledge the support of Unilever Research & Development, Trumbull, CT, and of EU COST Action D43 for this study. The authors are thankful to Prof. I.B. Ivanov for the stimulating discussions.

References

[1] R.G. Bartolo, M.L. Lynch, Kirk-Othmers Encyclopedia of Chemical Technologies, fourth ed., Wiley, New York, 1997.
[2] M.R. Porter, Handbook of Surfactants, Blackie Academic & Professional, London, 1997.
[3] M.L. Lynch, F. Wireko, M. Tarek, M. Klein, J. Phys. Chem. B 105 (2001) 552–561.
[4] J. Lucassen, J. Phys. Chem. 70 (1966) 1824–1830.
[5] P. Ekwall, W. Mylius, Ber. Deutsch. Chem. Ges. 62 (1929) 1080–1084.
[6] P. Ekwall, W. Mylius, Ber. Deutsch. Chem. Ges. 62 (1929) 2687–2690.
[7] P. Ekwall, Z. Anorg. Allg. Chem. 210 (1933) 337–349.
[8] J.W. McBain, M.C. Field, J. Phys. Chem. 37 (1933) 675–684.
[9] J.W. McBain, M.C. Field, J. Chem. Soc. (1933) 920–924.
[10] P. Ekwall, Kolloid-Z. 92 (1940) 141–157.
[11] P. Ekwall, L.G. Lindblad, Kolloid-Z. 94 (1941) 42–57.
[12] P. Ekwall, Colloid Polym. Sci. 266 (1988) 279–282.
[13] M.L. Lynch, Y. Pan, R.G. Laughlin, J. Phys. Chem. 100 (1996) 357–361.
[14] M.L. Lynch, Curr. Opin. Colloid Interface Sci. 2 (1997) 495–500.
[15] X. Wen, E.I. Franses, J. Colloid Interface Sci. 231 (2000) 42–51.
[16] X. Wen, J. Lauterbach, E.I. Franses, Langmuir 16 (2000) 6987–6994.
[17] J.R. Kanicky, D.O. Shah, Langmuir 19 (2003) 2034–2038.
[18] A.M. Saitta, M.L. Klein, J. Chem. Phys. 118 (2003) 1–3.
[19] M. Heppenstall-Butler, M.F. Butler, Langmuir 19 (2003) 10061–10072.
[20] S. Zhu, M. Heppenstall-Butler, M.F. Butler, P.D.A. Pudney, D. Ferdinando, K.J. Mutch, J. Phys. Chem. B 109 (2005) 11753–11761.
[21] P.A. Kralchevsky, K.D. Danov, C.I. Pishmanova, S.D. Kralchevska, N.C. Christov, K.P. Ananthapadmanabhan, A. Lips, Langmuir 23 (2007) 3538–3553.
[22] P.A. Kralchevsky, K.D. Danov, M.P. Boneva, S.D. Kralchevska, K.P. Ananthapadmanabhan, A. Lips, Adv. Colloid Interface Sci. (2008), in preparation.
[23] W. Jiang, J. Hao, Z. Wu, Langmuir 24 (2008) 3150–3156.
[24] P. Walden, E.J. Birr, Z. Phys. Chem. A 144 (1929) 269.
[25] P. Walden, H. Gloy, Z. Phys. Chem. A 144 (1929) 395.
[26] H.S. Harned, B.B. Owen, The Physical Chemistry of Electrolytic Solutions, second ed., Reinhold Publishing Corp., New York, 1950.
[27] F. Kohlrausch, On the conductivity of electrolytes dissolved in water in relation to the migration of their components, Paper presented before the Göttingen Academy of Sciences, May 6, 1876.
[28] A.N. Campbell, G.R. Lakshminarayanan, Can. J. Chem. 43 (1965) 1729–1737.
[29] Y. Zimmels, I.J. Lin, Colloid Polym. Sci. 252 (1974) 594–612.
[30] R.P. Varma, H. Goel, Colloids Surf. A 85 (1994) 69–73.
[31] L. Onsager, R.M. Fuoss, J. Phys. Chem. 36 (1932) 2689–2778.
[32] F. Daniels, R.A. Alberty, Physical Chemistry, fourth ed., Wiley, New York, 1975.
[33] R.A. Robinson, R.H. Stokes, Electrolyte Solutions, second ed., Butterworths, London, 1965.
[34] A.A. Ravdel, A.M. Ponomareva (Eds.), Concise Handbook of Physiochemical Quantities, eighth ed., Khimiya, Leningrad, 1983 [in Russian].